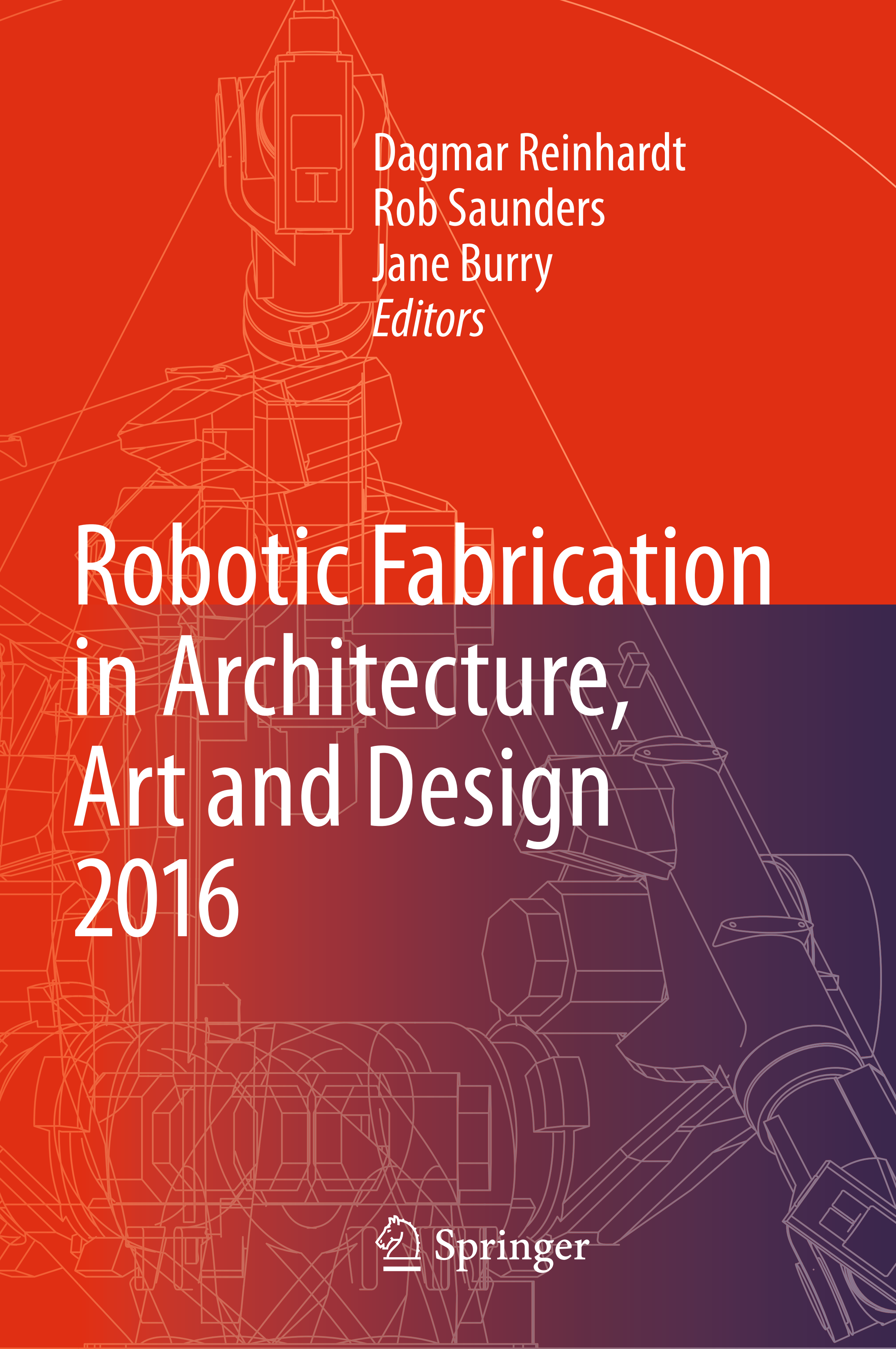

Dagmar Reinhardt
Rob Saunders
Jane Burry
Editors

Robotic Fabrication in Architecture, Art and Design 2016

Springer

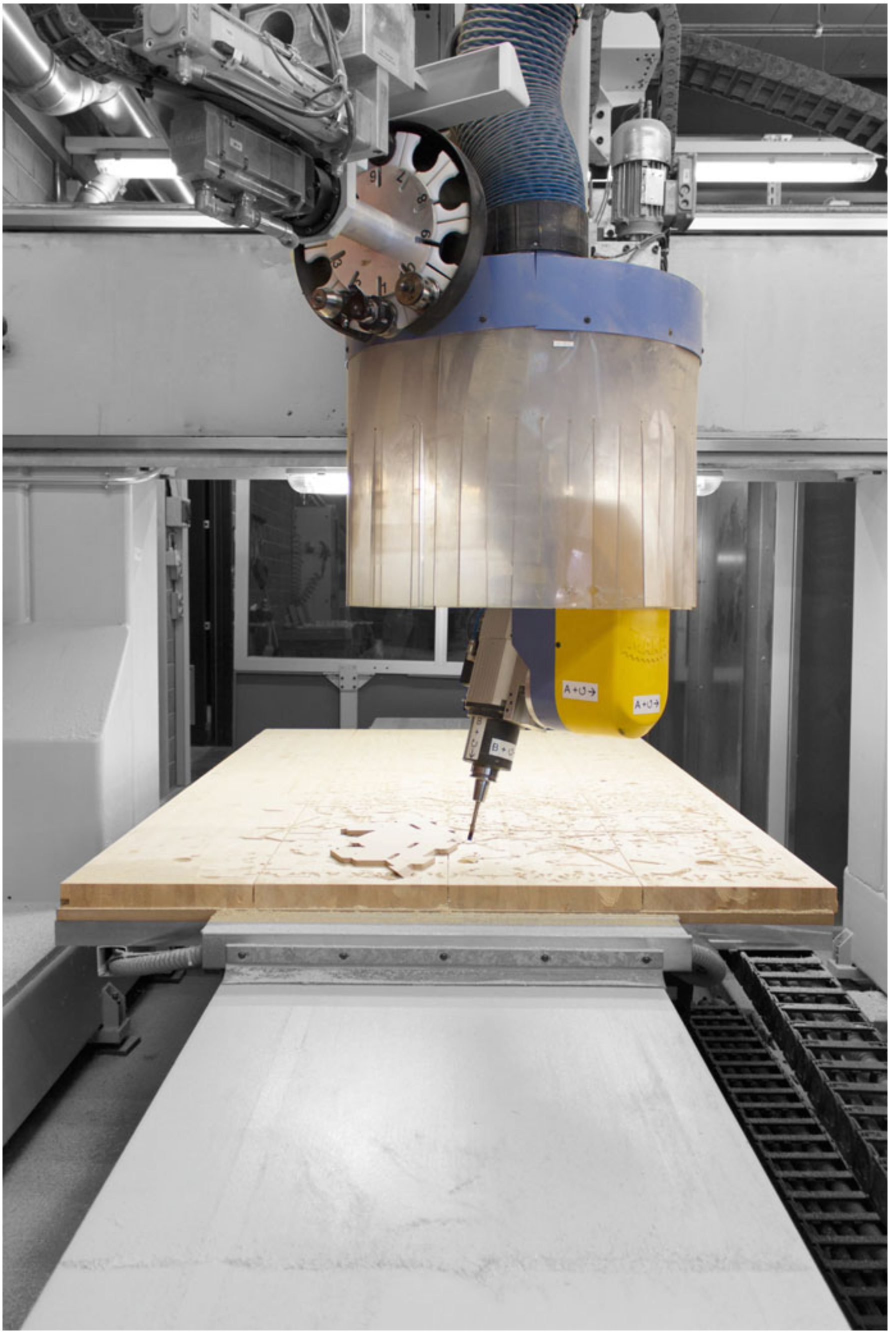

Fabrication-Aware Design of Timber Folded Plate Shells with Double Through Tenon Joints

Christopher Robeller and Yves Weinand

Abstract Integral attachment, the joining of parts through their form rather than additional connectors or adhesives, is a common technique in many industry sectors. Following a renaissance of integral joints for timber frame structures, recent research investigates techniques for the attachment of timber plate structures. This paper introduces double through tenon joints, which allow for the rapid, precise and fully integral assembly of doubly-curved folded surface structures with two interconnected layers of cross-laminated engineered wood panels. The shape of the plates and the assembly sequence allow for an attachment without additional connectors or adhesives. The fabrication and assembly constraint based design is achieved through algorithms, which automatically generate the geometry of the parts and the G-Code for the fabrication. We present the fabrication and assembly of prototypes fabricated with 3D CNC milling and laser cutting systems, comparing and discussing the advantages and disadvantages of the individual techniques.

Keywords Folded surface structures · Integral attachment · Laminated veneer lumber · Miura ori fold · 5-axis CNC · 2D/3D laser cutting

1 Introduction

In the design of smooth segmented plate shells, methods such as the Tangent Plane Intersection TPI (Troche 2008) can be used for the panelization of doubly-curved freeform surfaces. Different methods are required for the design of irregular and freeform folded surface structures. Previous techniques have been presented using triangulations (Trautz and Buelow 2009) and Origami inspired techniques using

C. Robeller (✉) · Y. Weinand
Timber Construction Laboratory IBOIS, EPFL Lausanne, Lausanne, Switzerland
e-mail: christopher.robeller@epfl.ch

Y. Weinand
e-mail: yves.weinand@epfl.ch

D. Reinhardt et al. (eds.), *Robotic Fabrication in Architecture, Art and Design 2016*, DOI 10.1007/978-3-319-26378-6_12

reflection planes and cross-section profiles (Buri and Weinand 2006) or mathematical models (Tachi 2009).

In parallel, research is being undertaken for the construction of shells with lightweight and sustainable timber plates using laminated veneer lumber (LVL). The easy machining of wood combined with numerically controlled machines allows for the integration of joints into the geometry of the plates, allowing for a rapid and precise assembly, aesthetic and easy-to-recycle mono-material structures (Robeller 2015).

This paper builds upon previous research in the field and presents a new method that integrates fabrication and assembly constraints specific to folded surface structures built from LVL panels and assembled with integral attachment techniques.

2 2-Layer Assembly with Through Tenon Joints

Integral multiple-tab-and-slot joints (MTSJ) such as finger joints provide geometric features for a fast and precise alignment and assembly of the plates, as well as a high resistance to compression and shear (Roche et al. 2015b), which are the primary forces in segmented and folded timber plate structures. However the joints between the plates receive not only shear, but also traction and bending forces. These forces are typically supported by metal connectors. Alternative solutions are hybrid finger/screw joints, such as in the ICD/ITKE LaGa Shell (Krieg et al. 2014) or prismatic integral joints such as dovetails, which provide additional features for the assembly and a resistance to bending and traction forces.

A comparison of the bending moment resistance of different edgewise joints for laminated veneer lumber (LVL) plates has recently been provided by the authors (Roche et al. 2015a), including screwed-, finger-, dovetail-, nejiri arigata- and through tenon joints. This comparison showed that the strength of the through tenon joints was the highest, which comes at the cost of a short protrusion beyond the jointed corners.

A design constraint of the through tenon joints is their restriction to connections of plates in two planes. A connection of plates in one plane is impossible due to the joint geometry. In consequence, these joints are not applicable to smooth manifolds, however they can be used for the design of folded timber plate structures. In these designs, plates are always connected in two planes, where an orthogonal dihedral angle $\varphi = 90^\circ$ between the plates is beneficial for the structural performance as well as for the fabrication process (Fig. 1).

However, a deviation β from this orthogonal angle is required for the design of curved and irregular shell structures. When using through tenon joints, β is equivalent to the inclination of the cuts, which are required for the fabrication of the joints. Such cuts can be fabricated with multi-axis cutting machines such as gantry or robot routers or laser cutters, however the inclination β_{max} of these machines is limited, which sets a hard fabrication-constraint that must not be exceeded anywhere in the design.

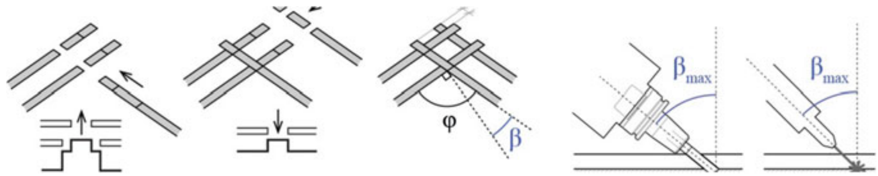

Fig. 1 Fully integral 2-layer assembly with double through tenon joints (*left*); fabrication constraints (*right*)

Figure 1 shows the through tenon joints ability to connect to multiple adjacent plates through intersection. An entirely integral attachment of four plates is possible following the illustrated method. On a mountain fold (as illustrated) the lower plate intersects both counterparts with a double through tenon joint. Then, the upper plate is inserted onto the tenons on its counterparts like a splice plate, which we call inverse assembly. On a valley fold, the upper plate is inserted with a double-tenon and the lower plate is inserted inversely. Major benefits of this connection include:

1. A direct connection of the lower layers to the upper layers, without transferring the forces through additional elements such as connectors.
2. Integral spacing of the two layers, which are kept at the correct distance
3. Blocking of elements: In such an assembly, only the last segment (two plates) can be removed. All other plates are blocked and firmly held in place by other parts, which must be removed before. A disassembly is only possible in the reversed piecewise order of assembly. Therefore, no additional connectors are required to fix the plates. This does not only bring aesthetic advantages, rapid assembly and cost savings, but it also allows the use of thin plates, on which the use of edgewise screwed joints may not be permitted (DIBt 2011).

3 Segmentation of Doubly-Curved Folded Plate Shells

For the construction of self-supporting, doubly-curved surface structures with discrete plate elements, we must find a segmentation that satisfies the previously mentioned constraints. Figure 2 illustrates this procedure on a target surface with a span of 10 m in the V-direction and a span-to-rise ratio of 3.

In a first step we discretize this surface into quadratic quadrilateral polygon mesh faces. The resulting value $\beta_{mean} = 85.6°$ indicates that we cannot join the plates with through tenon joints, because our 3D cutting techniques are limited to $\beta_{max} = 45°$.

Instead, we will use two folding patterns known from Japanese Origami paper folding:

Pattern 1, Yoshimura Fold Pattern, is a triangulation of the previous quadrilateral mesh. The deviation β is still very large, but can be reduced through a reduction of

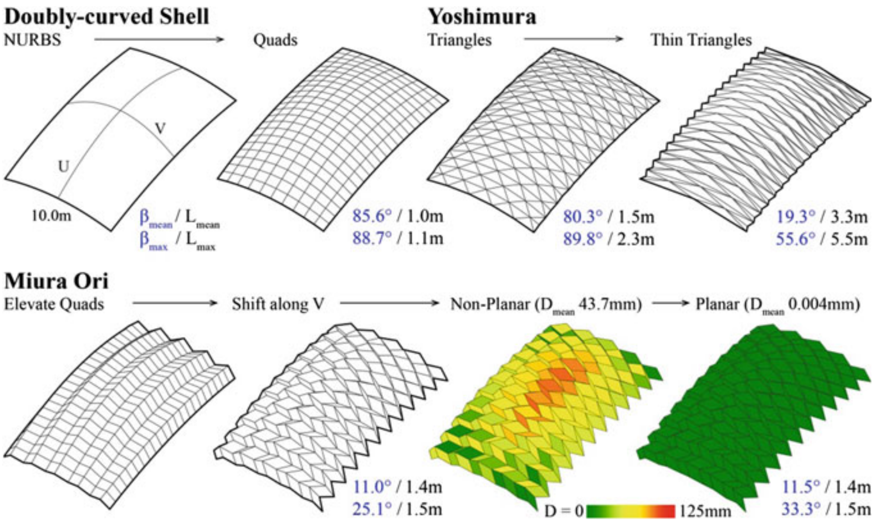

Fig. 2 Constraint-based segmentation of a doubly-curved target surface

segments in the V-direction. This results in deformed thin triangles (Fig. 2, top right) and large plates with $\boldsymbol{L_{max}}$ being larger than 1/2 of the span of the structure. The assembly of such large parts with integral joints is difficult, because the edges of the plates must be kept parallel during the insertion of the joints.

Pattern 2, Miura-Ori Pattern, presents an alternative approach. While previous Origami-related methods aim at flat-foldable designs, we plan to produce our structure from discrete components and do not include a flat-foldability constraint. Instead, we generate a pattern through the evaluation of a point grid on the parametric base surface, where every second vertex in the U-direction is shifted by a half segment length along V, and every second vertex in the V-direction is raised by the offset length h along the surface normal. With this method, we can reduce the global deviation β_{mean} to 11° at an offset height of $h = 0.75$ m, which satisfies the fabrication constraints of our 3D cutting methods. However the quadrilaterals generated with this method are not fully planar. D denotes the closest distance between face diagonals. We reduce D_{mean} to 0.004 mm in a second step using an external optimization framework (Bouaziz et al. 2012), which flattens the faces while it preserves the surface boundary. β_{max} increases slightly through this step, which could be reduced through an integration of the dihedral angle constraint into the external optimization framework. However, the solver cannot find a fold pattern that satisfies the dihedral angle constraints without an initialization mesh with the correct mountain and valley folds. Therefore we have chosen our strategy in two separate steps.

4 Algorithmic Joint Generation

From the Miura-Ori based segmentation we obtain 432 individually shaped quadrilaterals with 1,728 edges with different dihedral angles that must be joined. Numerically controlled fabrication technology allows for the rapid fabrication of these individually shaped plates, however the generation of the joints, as well as the machine code must be generated with an algorithm.

4.1 Assembly Order and Joint Configuration

We base our algorithm on a polygon mesh with a uniform sampling of the unit circle (Fig. 3a). Figure 3b shows that for each plate, up to 2 edges must be joined simultaneously. The common insertion direction v for these edges is found at their bisector. This causes a deviation θ from a line on the plane perpendicular to the edge. It is assembly-constrained to $\theta_{max} = \pm 30°$. A piecewise assembly of our structure is only possible as illustrated, with the x-direction changing in every second row (due to the opposite obtuse angles of the faces changing in every second row in the Miura Ori pattern). In Sect. 2 the tab-and-slot configuration was described, as well as its inversion based on mountain and valley folds.

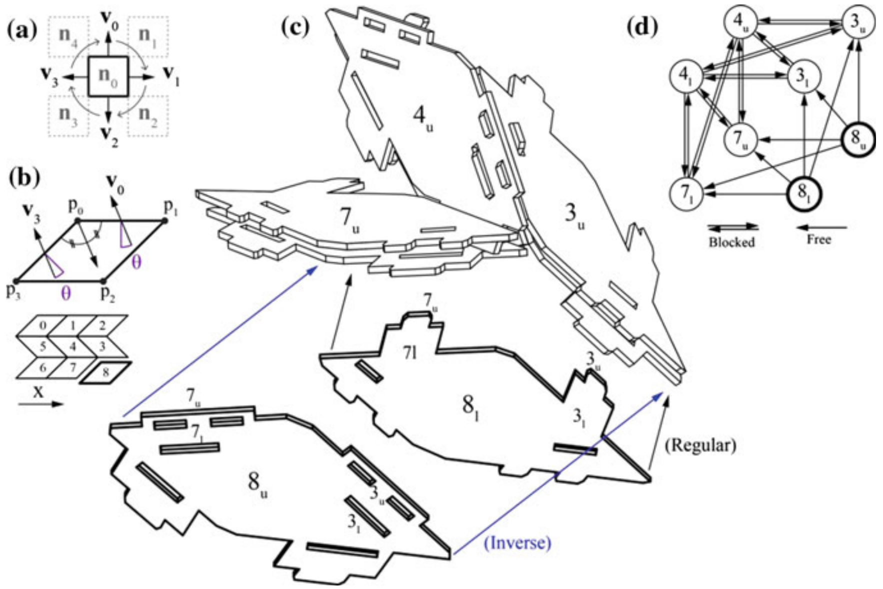

Fig. 3 **a** Assembly order, **b** blocking graph, **c** insertion vectors

Table 1 Joint processing and 2D cut adaptation for Fig. 2 and t = 3 mm, o = 4*t

Joint configuration				Tenon rotations			2D cut adaptation		
Plate	Edge	a	Joint config.	φ	β	θ	l_{tenon}	w_{slot}	l_{slot}
28-1	0	0.96	1 double through tenon	67.04	13.96	29.69	13.8	3.84	13.71
28-1	1	−1	2 through tenons	90.5	0.5	29.6	13.79	3.03	13.7
28-1	2	−0.94	2 through tenons	73.34	16.66	20.6	13.38	4.03	13.13
28-1	3	0.99	1 double through tenon	99.55	9.55	19.61	12.65	3.55	13.07
28-2	0	0.96	None						
28-2	1	−1	1 double through tenon	90.5	0.5	29.6	13.79	3.03	13.7
28-2	2	−0.94	1 double through tenon	73.34	16.66	20.6	13.38	4.03	13.13
28-2	3	0.99	None						

On the polygon mesh, we identify mountain and valley folds per edge, using the normals n_i, n_j of the two adjacent faces and the vertices p_k, p_l of their shared edge: $a = \left(n_i \times n_j\right) \cdot \left(\widehat{p_k - p_l}\right)$. From this we obtain $a > 0$ or $a < 0$, indicating mountain or valley folds and therefore the correct joint configuration (Fig. 3c, Table 1).

4.2 Insertion Directions

In addition to the two simultaneously assembled edges with outgoing through tenons (v_0 and v_1 in the positive x-direction and v_0 and v_3 in the negative x-direction), the tenons on the other two edges connect to inversely inserted incoming parts, such as plate 8u, Fig. 3c, which connects to the four plates 3u,3l,7u,7l simultaneously. Here, the only possible insertion direction is found at the intersection line between the plates 3 and 7. Generally, all insertion directions for incoming, inversely assembled parts are determined through a cross product with the face normals of the diagonal neighbours in the direction of assembly: If a row is assembled in the positive x-direction, $v_3 = n_0 \times n_4$ and $v_2 = n_0 \times n_3$. In the negative x-direction the incoming through tenon directions are $v_2 = n_0 \times n_2$ and $v_1 = n_0 \times n_1$.

4.3 Connectivity and Blockings

Generally joints in timber constructions are semi-rigid, introducing a certain weakness in the structure. Apart from improving the strength of the joints, it is beneficial to attach each plate to multiple adjacent plates. In a regular single-layer assembly with quadrilaterals, each plate is connected to 4 adjacent plates, in the 2-layer folded structure with through tenon joints, each plate is attached to 8 adjacent plates. For example, plate 4_u in Fig. 3b, c connects to 1_u, 1_l, 3_u, 3_l, 7_u, 7_l, 5_u, 5_l.

The mutual blocking of parts is illustrated in a so called Blocking Graph (Wilson and Latombe 1994) in Fig. 3d. It shows that the pieces 4_l and 4_u are blocking all other parts in the assembly. Due to the individual insertion directions (about 1,500 individual directions in Fig. 2), it is impossible to detach an entire row or column of elements. The through tenon joints perform like diagonally, crosswise applied screws.

5 Prototype Fabrication

5.1 Milling System

Figure 4 shows an arch prototype (based on a single-curvature target surface) connected only with through tenon joints, built to test the fabrication, assembly and the stiffness of the resulting structure system. The prototype with a span of 3.250 mm, a width of 295 mm and a weight of 82 kg was built from 9-layer birch plywood panels with a thickness of $t = 12\,\text{mm}$. The offset between the plates along the face normal was set to $o = 4 * t$. With a span-to-rise-ratio of 9, the arch demonstrates the construction of a shell with a low curvature like in a typical roof structure. The maximum tool inclination for the joint fabrication is reduced to $\beta_{max} = 11.5°$.

The parts were fabricated with a 5-axis gantry router equipped with a 10 kW electro spindle, operated at 16.000 rpm and a feed rate of 5 m/min in 2 vertical infeeds. The G-Code for the fabrication was generated with a custom script, based on a Loft—type synchronization between upper and lower polygon outlines of the

Fig. 4 Prototype assembled only with through tenon joints

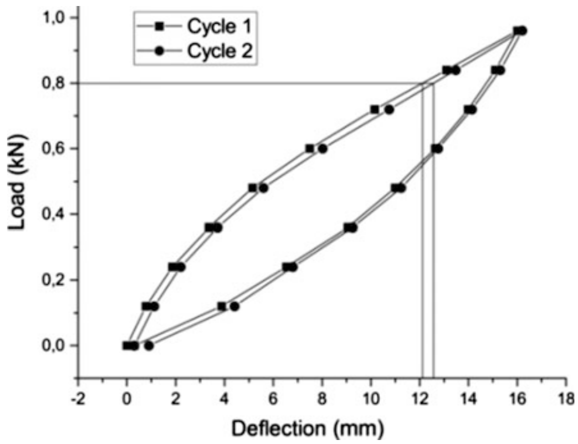

Fig. 5 Load test for Fig. 4

plates and a conversion of the 3D tool vector into cardan rotations using an arctangent function with two arguments. All joints and slots were cut without additional gaps or tolerances. The tight fitting pieces were inserted quickly and precisely, the insertion force was applied with a rubber mallet.

Figure 5 shows an experimental load test that was performed on this prototype. A load of up to 0.84 kN was first applied and then removed in eight steps of 120 N. This cycle was repeated two times. applying a load of 0.8 kN, which is equivalent to the self-weight of the structure, a vertical deflection of 12.1 mm (Cycle 1) and 12.3 mm (Cycle 2) was measured at the center point.

5.2 *Laser Cutting System*

For the production of small-scale prototypes of doubly curved shells with medium density fiberboard (MDF) and construction paper, laser cutting proved to be an efficient technique. However, widely available 2D laser systems cannot cut angular slots for our through tenon joints with two rotations β and θ. In the automated production of furniture with 3-axis milling machines, non-orthogonal joints are often realized through an increased slot width, which allows the inserted part to rotate to its predetermined rotated position. The contact between the two parts is along the edges of the slot rather than its side faces. We have integrated this method into the joint generation algorithm. Table 1 shows the joint processing for one of the segments (from Fig. 2), 8 edges are being processed on the upper and lower plate.

The first four columns show the joint configuration and the assignment of slots to the adjacent plates, followed by the dihedral angle and the joint rotations. From these rotations, as well the thickness t and the offset o, we can calculate corrections

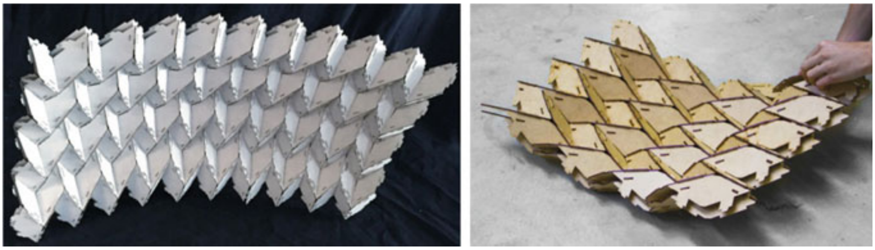

Fig. 6 Doubly-curved 2-layer shell, fabricated with a 2D laser cutter

for the shortening of the tenon base l_{tenon}, the extension of the slot width w_{slot}, and the extension of the slot length l_{slot}.

$$\boldsymbol{l_{tenon}} = \frac{\frac{o}{\cos\beta} - \tan\beta * \left(\frac{t}{2}\right)}{\cos\theta} \quad w_{slot} = \frac{t}{\cos\beta} + t * \tan\beta \quad l_{slot} = w_{tenon} + t * \tan(\theta)$$

This method allows for the rapid production of precise 3D models based on doubly curved target surfaces. Figure 6 shows two of the smaller prototypes that we have built with 3 mm MDF and 1 mm construction paper.

5.3 3D Laser System

Due to the contactless operation of laser cutting systems, there is a constant cut quality, no tool wear and the multi-axis robot or gantry system is not exposed to mechanical forces generated by the cutting. The resulting ease—and rapidity of production of this method raises the question whether it could also be used for full-scale applications. Additionally, larger-scale laser systems in the automotive industry are commonly used for the trimming of deep-drawn, curved sheets of hardened steel and therefore capable of 3D simultaneous cutting (illustrated in Fig. 1), similar to the 3D milling system used in Sect. 5.1. We have performed tests with such a system, cutting through tenon joints and slots on structural grade spruce LVL panels with a thickness of up to $t = 38$ mm and a 3D rotation of up to $\beta = 45°$ using a gantry machine equipped with a 6 kW CO_2 laser. Cutting at a feed rate of 11 m/min (in a single infeed) with N_2 gas and 5 kW power, the accuracy of the joints was high and independent from the rotation β. The cut width of only 0.6 mm allows for thin cuts and small radii on corners in the cutting contours. However, a disadvantage of the method is the charring and odor of the laser-cut edge surfaces. This can be decreased through higher feed rates but remains noticeable.

6 Conclusion

Through tenon joints for LVL panels combine the shear strength of finger joints with a high resistance to bending moments and out-of-plane traction. The prototypes presented in this paper demonstrate the additional possibility of using double through tenon joints for the integral attachment and spacing of double-layered timber plate structures.

The plate configuration based on the Miura-Ori pattern allows for the design of fabrication- and assembly-aware doubly curved folded surface structures. While the Yoshimura pattern is constrained to target surfaces with a high curvature and results in large plate sizes, the Miura-Ori pattern can also be applied to surfaces with a low curvature. However, the vertical elevation of the vertices in the Miura-Ori also results in certain structural disadvantages (Stitic et al. 2015). Further research is necessary to determine if the structurally advantageous shape of the Yoshimura pattern outweighs the disadvantages in its fabrication, joining and assembly.

Clear advantages of the joint configuration and assembly sequence described in Sect. 4 include the direct connection of each plate to 8 adjacent plates, as well as the mutual blocking of the plates which only allows for a piecewise disassembly in the reverse order of assembly. Therefore, a traction resistance of the joints is not required and additional connectors such as screws, metal plates or adhesives are not necessary.

The production of prototypes with 3D milling as well as 2D and 3D laser cutting systems has shown advantages and disadvantages of the individual solutions. The highest quality cuts on LVL plates can be achieved with saw blades, due to the large diameter and the large number of blades. However the production of the concave polygonal contours and slots of the through tenon joints is not possible with such tools. Instead, we have used milling bits with a radius of 6 mm, which allowed for the production of precise parts. The tight fit and precision of the joints was confirmed by a load-test of the arch prototype.

An alternative solution was presented for the fabrication of small-scale prototypes using a geometric adaptation of the joints for 2D laser systems. The method allows for the rapid production of precise models, however the plates are only in contact along lines, not surfaces. Further research is required analyzing the influence of this method on load-bearing joints. Finally, the advantages of the 3D milling and the 2D laser cutting were combined using a 3D laser system for the production of through tenon joints on structural grade LVL panels.

Acknowledgments The Authors would like to thank Franck Dal-zotto, Anders Holden Deleuran and TRUMPF Laser Technology. This research was supported by the Swiss National Competence Center in Research (NCCR) Digital Fabrication.

References

Bouaziz, S et al., 2012, ‘Shape-up: Shaping Discrete Geometry with Projections’, in Computer Graphics Forum, vol. 31, pp. 1657–1667. Wiley Online Library.

Buri, H and Weinand, Y 2006, ‘BSP Visionen -Faltwerkkonstruktionenaus BSP-Elementen’ in Grazer Holzbau-Fachtage, Verlag der TechnischenUniversität Graz, Graz.

DIBt 2011, Allgemeine bauaufsichtliche Zulassung Kerto-Q Z-9.1-100, Paragraph 4.2 and Attachment No 7, Table 5. Deutsches Institut für Bautechnik.

Krieg O, Schwinn T, Menges A, Li J, Knippers J, Schmitt A, Schwieger V 2014, ‘Computational integration of robotic fabrication, architectural geometry and structural design for biomimetic lightweight timber plate shells’, in Advances in Architectural Geometry 2014. Springer Verlag, London

Robeller, C 2015, Integral Mechanical Attachment for Timber Folded Plate Structures, PhD thesis, EPFL ENAC, Lausanne, Switzerland.

Roche, S, Mattoni, G, Weinand, Y 2015a, ‘Rotational stiffness at ridges in folded plate structures’, in Elegance of Structures: IABSE-IASS Symposium 2015, Nara, Japan.

Roche, S, Robeller, C, Humbert, L, Weinand, Y 2015b, ‘On the Semi-Rigidity of Dovetail Joint for the Joinery of LVLPanels’, European Journal of Wood and Wood Products, pp. 1-9.

Stitic, A, Robeller, C, Weinand, Y 2015, ‘Form Exploration of Folded Plate Timber Structures Based on Performance Criteria’, in Elegance of Structures: IABSE-IASS Symposium, 2015, Nara, Japan.

Tachi, T 2009, ‘Simulation of Rigid Origami’, Origami, no. 4, pp. 175-187.

Trautz, M and Buelow, P 2009, ‘The Application of Folded Plate Principles on Spatial Structures with Regular, Irregular and Free-Form Geometries’, in IASS – Evolution and Trends in Design, Analysis and Construction of Shell and Spatial Structures, Valencia.

Troche, C 2008, ‘Planar Hexagonal Meshes by Tangent Plane Intersection’, in Advances in Architectural Geometry 2008, Springer, Vienna.

Wilson, R and Latombe, J 1994, ‘Geometric Reasoning about Mechanical Assembly’, Artificial Intelligence, vol.71, no.2, pp. 371-396.